Biases Affecting the Measurements of Tumor-to-Background Activity Ratio in PET

M. Soret, C. Riddell, S. Hapdey, and I. Buvat

***Abstract*—The influence of various factors on the biases affecting tumor-to-background activity ratio (TBR) estimates in positron emission tomography (PET) was studied using analytical simulations of an anthropomorphic phantom. The impact of attenuation correction (AC) on TBR as a function of tumor location and tumor-to-background density ratio was studied. The TBR changes that would be observed when a tumor with uniform uptake turns to a tumor with nonuniform uptake due a necrotic process were characterized. Major parameters affecting the bias in TBR estimates were the tumor diameter, the TBR, whether AC had been performed and the spatial resolution of the PET scanner. Our results suggest that a necrotic process gets detectable if the necrotic volume is at least 50% of the total tumor volume for a necrosis-to-tumor activity ratio of 0.5. We discuss how our results regarding TBR biases translate into standardized uptake values biases.**

***Index Terms*—Attenuation, measurement, partial volume effect, positron emmission tomography (PET), standardized uptake value, tumor.**

I. Introduction

ACCURATE estimates of tumor uptake in flouro-deoxyglucose (FDG) positron emission tomography (PET) would be useful for lesion characterization and patient follow-up. However, tumor uptake measurements are challenging given the small size of many tumors and the limited spatial resolution in PET. A common index used to differentiate benign from malignant tumors is the tumor-to-background activity ratio (TBR) [1]–[3]. The effect of limited spatial resolution on activity estimates in small spheres surrounded by uniform background has already been studied in PET using simple geometric models [4], [5]. A controversial question in FDG PET is the clinical usefulness of attenuation correction (AC) [6]–[9]. Another relevant question concerns the ability of detecting small changes in tumor metabolism using FDG PET, as occur at the beginning of a necrotic process yielding nonuniform tumor uptake. To investigate these issues, we determined the effect of tumor diameter (D), TBR, attenuation, spatial resolution, tumor location and nonuniform tumor uptake on the biases affecting TBR estimates in PET using simulations of an anthropomorphic phantom.

Manuscript received April 23, 2001; revised July 23, 2002.

M. Soret, S. Hapdey and I. Buvat are with the U494 INSERM, CHU Pitié-Salpêtrière, Paris, France (e-mail: soret@imed.jussieu.fr).

C. Riddell was with the U494 INSERM CHU Pitié-Salpêtrière, Paris, France and is now with GE Medical System, Buc, France (e-mail: Cyril.Riddell@med.ge.com).

Digital Object Identifier 10.1109/TNS.2002.803687

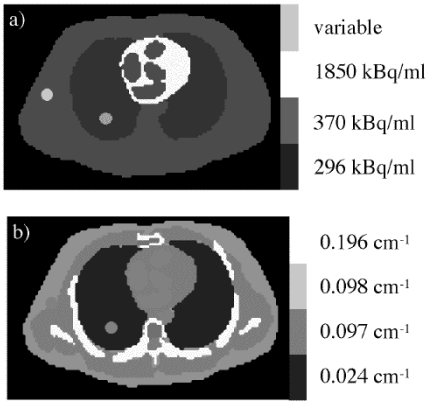

Fig. 1. Examples of axial slices through: (a) the simulated activity distribution; (b) the attenuation distribution.

II. Material and Methods

Three-dimensional *(3-D) numerical phantom*. Various factors potentially affecting tumor uptake measurements in PET were studied by performing analytical simulations using the 3-D numerical Zubal thoracic phantom [10] sampled with 1 mm $\times$ 1 mm $\times$ 1 mm voxels. Activity and attenuation distributions were defined to respect anatomical and physiological properties (Fig. 1). Realistic FDG activity concentrations were set in the heart (1850 kBq/ml), lungs (296 kBq/ml) and soft tissues (370 kBq/ml). Two spheres representing tumors were added in the lungs and soft tissues to investigate the impact of tumor location. Attenuation coefficients at 511 keV were set to 0.099, 0.024, 0.098 and 0.097 cm^{-1} in tumors, lungs, muscle, and heart, respectively.

Analytical noise-free simulations. Noise-free emission projections with or without attenuation medium were simulated. Each simulation resulted in 40 sinograms corresponding to 40 transaxial slices, each sinogram including 300 angular samples and 512 projection bins. Projection bin spacing and axial sampling were 1 mm each. The point spread function (PSF) of the PET system was modeled by convolving the simulated data with a 2D Gaussian function (along the projection bins and in the axial direction) of full width at half maximum (FWHM) equal to 4 mm. Transmission data were blurred using the same PSF.

The attenuated emission projections were corrected for attenuation by multiplying the sinograms by the AC factors derived from the noise-free transmission simulations. Images were reconstructed using the Ordered Subset Expectation Maximization (OSEM) algorithm (16 subsets, four iterations)

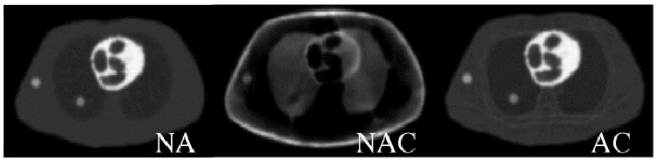

Fig. 2. Reconstructed activity distribution corresponding to NA, NAC, and AC.

[11], yielding ten slices 128×128 with 4 mm $\times$ 4 mm $\times$ 4 mm voxels. Spatial resolution in the reconstructed images was around 6.5 mm.

Effect of tumor diameter and TBR. To study the effect of tumor diameter (D) upon the bias in TBR measurements, simulations involving tumors with diameters D of 0.5, 1, 1.5, 2, 3, and 4 cm were performed. Tumor-to-surrounding tissue (background) uptake ratios were varied from 3 to 13.

Effect of attenuation. Three data sets were obtained to investigate the effect of attenuation: data without simulating any attenuating medium as if the photons propagated in air (NA), data with simulation of the attenuating media and without AC (NAC), and data with simulation of the attenuating media and AC (having AC) (Fig. 2). These three data sets were used to investigate the efficiency of AC by comparing NA with those having AC, and to study the impact of AC, by comparing NAC with those having AC.

Effect of spatial resolution. The influence of the PET system spatial resolution was studied by repeating the simulations with a system resolution of $\mathrm{FWHM} = 8$ mm instead of 4 mm. An 8-mm resolution is more representative of a gamma-camera based PET scanner than of a dedicated PET scanner [7]. These simulations were used to assess the impact of the PET system spatial resolution on quantitative performances. Influence of a PSF in transmission measurements (FWHM_T) different from the PSF in emission measurements $(\mathrm{FWHM}_E = 4$ mm$)$ was also studied in two cases: "smoothed" transmission data corresponding to $\mathrm{FWHM}_T = 8$ mm and CT transmission data corresponding to $\mathrm{FWHM}_T = 1$ mm.

Effect of nonuniform uptake in the tumor. Lung tumors with nonuniform uptake were simulated using two concentric spheres: the inner sphere representing necrosis had a volume V_N varying from 0.25 to 0.75 times the tumor volume V and had an activity A_N varying from 0 to 1 times the tumor activity A. Tumor volume was varied from 0.5 cm^3 $(D = 1$ cm$)$ to 113.1 cm^3 $(D = 6$ cm$)$. The background activity A_B and the tumor activity were also varied. These simulations were used to assess the quantitative changes that would be observed when a tumor with a uniform uptake turns to a tumor with a nonuniform uptake due to a necrotic process.

Quantitative index. Tumor uptake and associated TBR were estimated as follows. The reconstructed volume (ten slices with a 4 mm $\times$ 4 mm $\times$ 4 mm voxels) was resampled using trilinear interpolation to a 1 mm $\times$ 1 mm $\times$ 1 mm voxel size identical to the sampling of the original activity distribution. For each resampled image, the tumor uptake was measured in a region of interest (ROI) corresponding to the anatomical region used to define the original activity distribution (1 mm $\times$ 1 mm $\times$ 1 mm voxel size). The background uptake was measured in an ROI of the same shape and size located in the contralateral region at a position mirroring the tumor location. TBR was estimated as the ratio of the mean value in the tumor ROI over the mean value in the background ROI. Percent errors affecting TBR estimates were defined as

$$100^* \frac{\text{estimated TBR} - \text{true TBR}}{\text{true TBR}}.$$

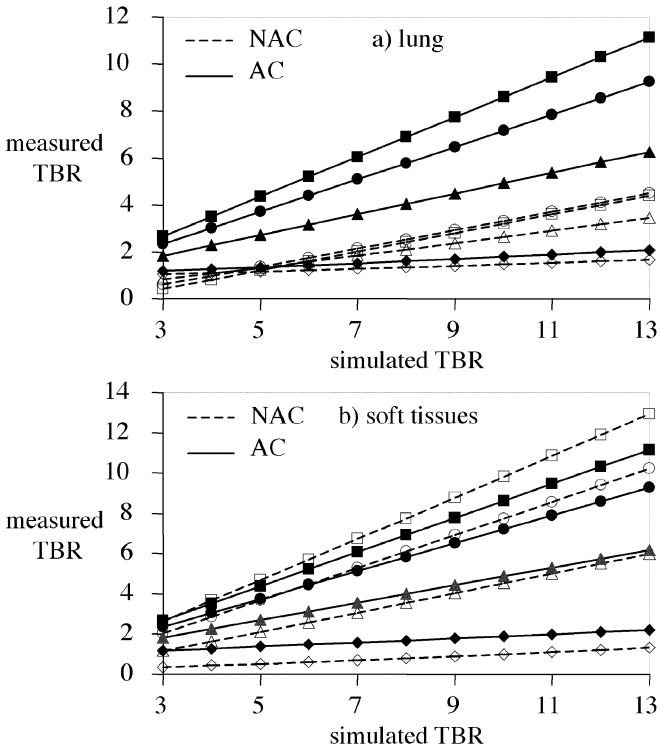

Fig. 3. Measured TBR in (a) lung tumor; (b) soft-tissue tumor with or without AC as a function of simulated TBR for lesion diameters of 4 cm (■), 2 cm (●), 1 cm (▲) and 0.5 cm (◆).

III. Results and Discussion

A. Effect of Tumor Diameter

Fig. 3 shows that the smaller the tumor diameter, the greater the underestimation (expressed as a percentage of the true TBR) of TBR, irrespective of AC. When the true TBR changed from 10 to 5 (50% decrease), the observed TBR reduction was 49% for a 4-cm–diameter tumor but was only 25% for a 0.5-cm-diameter tumor. When both tumor and background activities varied but TBR remained unchanged, observed TBR remained almost constant. For instance, for $\mathrm{TBR} = 6.5$ with 592 kBq/ml in the background and $D = 4$ cm, observed TBR was 5.25, while for $\mathrm{TBR} = 6.5$ with 148 kBq/ml in the background, observed TBR was 5.31. Curves shown in Fig. 3 are, therefore, valid for a wide range of background activities.

These results demonstrate that partial volume effect (PVE) makes the bias affecting TBR estimates strongly dependent on tumor size. A well-known rule of thumb is that PVE correction is needed for tumor diameter less than 2 or 3 times the FWHM characterizing the spatial resolution [5], i.e., for tumors less than 2 cm in diameter for the 6.5-mm spatial resolution observed in our reconstructed images. Our results show that even

for a 4-cm diameter tumor, PVE introduces a bias of 10% to 15% depending on the true TBR. This is because tumor uptakes were measured by averaging pixel values in ROIs corresponding to the anatomical size of the tumor, while the rule of thumb is valid when one considers only the maximum pixel value within a given ROI.

In FDG-PET, a TBR value of five, has been found to provide optimal sensitivity and specificity to differentiate between benign and malignant lesions in patients with solitary lung lesion [12]. These results were obtained for for pulmonary lesions greater than 1 cm in diameter, and for a spatial resolution in the reconstructed images was 6.5 mm $\times$ 6.5 mm $\times$ 8 mm. Given our results, this threshold of 5 corresponds, for a spatial resolution of 6.5 mm in the reconstructed images, to a true TBR of 10.5 for a 1-cm-diameter tumor, of 6.5 for 2-cm-diameter and of 5.5 for a 4-cm diameter.

Correction of TBR underestimation introduced by PVE can be performed using recovery coefficients [1], [4], [5], [13], [14]. As the PVE bias strongly depends on tumor diameter, the appropriate recovery coefficients have to be determined for a given tumor diameter.

When the data are not corrected for attenuation, the rate with which TBR underestimation varies with tumor diameter strongly depends on whether the tumor is located in the lungs or soft tissues. This is because PVE interferes with attenuation, as will be explained in Section III-C.

B. Effect of TBR

Fig. 3 shows that the greater the TBR, the larger the TBR underestimation expressed as a percentage of the true TBR. Indeed, for TBR close to 1, the spill-out (tumor activity detected outside the tumor) almost compensates the spill-in (background activity detected inside the tumor). Large TBR results in large discrepancy between spill-in and spill-out, hence in higher percent error in tumor uptake estimates. The appropriate recovery coefficients for PVE correction in a specific configuration thus depend on the true TBR.

C. Effect of Attenuation

Efficiency of AC. The TBR estimated using the images reconstructed from the AC projections and from the NA projections were almost identical. The difference between TBR values obtained with NA and AC averaged 0.74% (standard deviation was 0.62%) over all tumor diameters and soft tissue lung tumors.

Yet, partial volume effect affected the transmission measurements through small tumors located in the lung: the smaller the tumor, the greater the underestimation of the attenuation coefficient. For instance, the tumor attenuation coefficient was underestimated by 33% for a 2-cm-diameter tumor and by 55% for a 1-cm-diameter tumor on the reconstructed transmission scan. This bias in attenuation coefficient value was observed only for tumors of density significantly different from the density of surrounding tissues (lung tumors) because for tumor density similar to background density (soft-tissue tumors), spill-in compensated spill-out. The bias affecting the attenuation coefficients of the lung tumors did not affect AC accuracy however, because the partial volume effect affecting transmission measurements similarly affected the attenuation factors in emission measurements. Thus, the partial volume effect affecting transmission measurements in PET does not introduce any bias during the subsequent AC, when the spatial resolution affecting the emission measurements is identical to that used for the transmission measurements. The case of a different spatial resolution in emission and in transmission is studied in Section III-D.

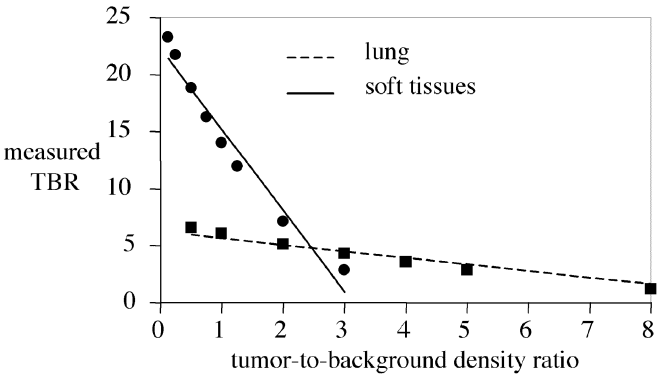

Fig. 4. Measured TBR without AC in a 4-cm tumor with true $\mathrm{TBR} = 13$ as a function of tumor-to-background density ratio in lung (■) and in soft tissues (•).

The excellent performance of AC reported in this study was obtained using noise-free emission and transmission measurements. The precise impact of the noise affecting both emission and transmission measurements on TBR estimates will be the subject of future studies.

Effect of AC. The change in TBR estimates introduced by AC varied depending on the tumor location. For lung tumors, TBR was greater with AC than without, while for soft-tissue tumors, the effect varied with the tumor diameter and with the true TBR (Fig. 3).

Without AC, TBR estimates are affected by attenuation and partial volume effect. With AC, TBR estimates are mostly biased by partial volume effect which depends on the tumor diameter and on the true TBR. Without AC, for fixed tumor location, the measured TBR depends on the ratio between tumor density and surrounding tissue density (Fig. 4). The higher this ratio, the greater the TBR underestimation.

The impact of attenuation on TBR not only depends on the tumor-to-background density ratio but also on the tumor location (Fig. 4): for identical tumor-to-background density ratios, a lung tumor and a soft-tissue tumor are not identically affected by attenuation as they are not located at the same position within the attenuating medium. Without AC, the smaller TBR measured for lung tumors compared to soft-tissue tumors is probably due to the fact that our simulated lung tumors were deeper inside the body than the soft-tissue tumors and were surrounded by different tissues. Without AC, true TBR are thus not predictable from the estimated TBR even if tumor size and tumor-to-background density ratio are known (Fig. 4). Recovery coefficients calculated for PVE correction are therefore not valid for images that are not corrected for attenuation since they depend on tumors location. After AC, this effect disappears and estimated TBR gets independent of both the tumor-to-background density ratio and the tumor location.

Our results regarding the impact of AC upon TBR estimates agree well with previously reported results [7] for a chest

phantom. This group found that the tumor contrast (defined as TBR—1) for lung tumors was higher with AC than without. However, they did not consider soft-tissue tumors.

A higher tumor contrast has been reported for images not corrected for attenuation compared to images corrected for attenuation in a phantom study involving a water attenuation medium [8]. This configuration was close to the one we studied when considering soft-tissue tumors with a tumor-to-background density ratio of 1. For a true TBR of 13, the measured TBR was 14 without AC, and 11 with AC, consistent with Bengel's findings [8]. In patient studies, this group also found that the TBR was significantly higher for images not corrected for attenuation compared to corrected images, regardless of lesion localization. These results disagree with ours regarding lung tumors. An explanation might be that in [8], transmission sinograms for AC were smoothed using a Gaussian filter, resulting in a better spatial resolution in the emission scan than in the transmission scan. In Section III-D, we demonstrate that for lung tumors, a lower spatial resolution in the transmission scan compared to that in the emission scan can introduce a larger TBR underestimation after AC than that observed for identical emission and transmission spatial resolutions. This could explain why in lung lesions, Bengel found lower TBR with AC than without.

Another clinical study [9] showed a significant difference in TBR between attenuation-corrected and uncorrected images in only 6 of 55 lesions (11%), located in mediastinum, lung, lymph nodes, bone, breast and adrenal. The changes in TBR without and with AC demonstrated that the impact of AC strongly depended on the tumor. This is consistent with our conclusion that the impact of attenuation depends on both tumor-to-background tissue density ratio and tumor location.

The different impact of AC depending on tumor-to-surrounding tissue density ratio and tumor location partially explains the current controversy regarding the benefit of AC for tumor detection [6]. Indeed, when AC decreases TBR (here, for soft-tissue tumors), lesions can get more difficult to detect after AC.

D. Effect of Spatial Resolution

Identical emission and transmission spatial resolution.

Changing the spatial resolution of the detector from 4 to 8 mm FWHM decreased the spatial resolution in reconstructed images from 6.5 to 9 mm. Such a change increased the tumor uptake underestimation from 52% to 66% for a 1 cm lung tumor with $\mathrm{TBR} = 13$. Whatever the tumor location, with AC, TBR was 1% to 30% lower with $\mathrm{FWHM} = 8$ mm than with $\mathrm{FWHM} = 4$ mm (Fig. 5). Indeed, the poorer the spatial resolution, the greater the biases introduced by PVE. For accurate quantitative measurements, recovery coefficients should also depend on spatial resolution.

Different emission and transmission spatial resolutions.

A difference between emission and transmission spatial resolutions has a substantial effect on measured TBR with AC for lung tumors only (Figs. 6 and 7): the better the transmission resolution, the smaller the biases affecting TBR. The respective spatial resolutions in emission and transmission scans thus only impact TBR measurements for tumors with a density different from that of the surrounding tissues. Indeed, when the

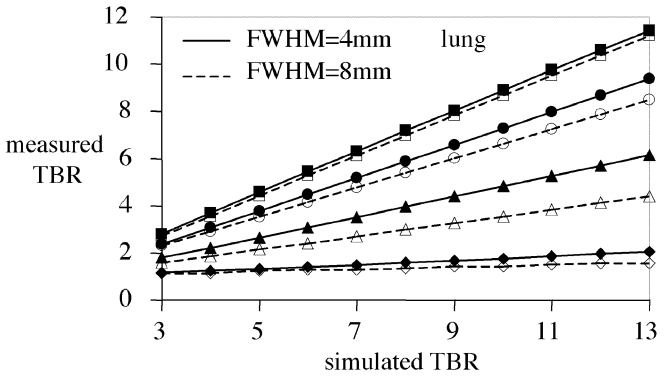

Fig. 5. Measured TBR with AC in a lung tumor with $\mathrm{FWHM}_{ET} = 8$ mm or $\mathrm{FWHM} = 4$ mm as a function of simulated TBR for lesion diameters of 4 cm (■), 2 cm (•), 1 cm (▲) and 0.5 cm (♦).

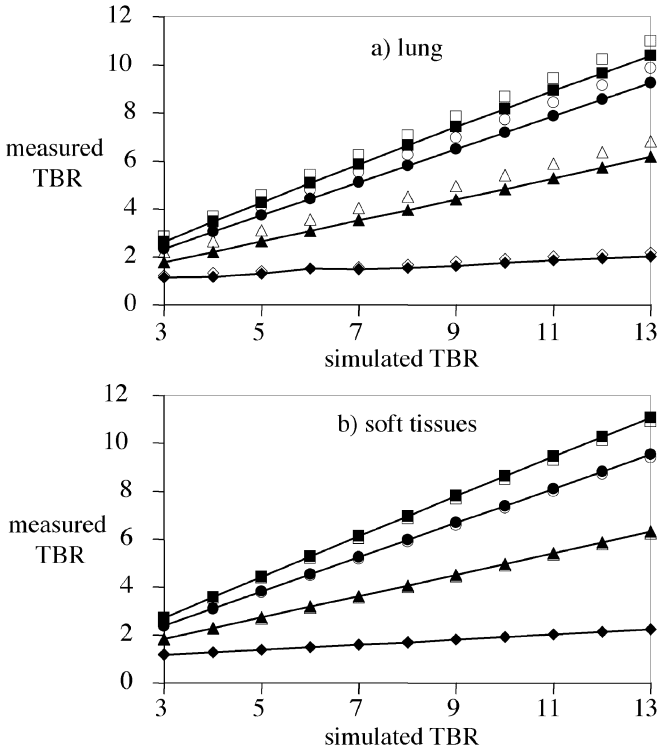

Fig. 6. Measured TBR with AC in (a) lung tumor; (b) soft-tissue tumor with $\mathrm{FWHM}_T = 1$ mm (empty symbols) and 4 mm (filled symbols) and $\mathrm{FWHM}_E = 4$ mm as a function of simulated TBR for lesion diameter of 4 cm (■), 2 cm (•), 1 cm (▲) and 0.5 cm (♦).

emission and transmission spatial resolutions are different, the PVE affecting the attenuation coefficient measurement during the transmission scan does not compensate exactly the PVE affecting the attenuation factors in the emission scan, as was observed for identical transmission and emission resolutions (see Section III-C). For lung tumors with a density greater than lung density, the better the transmission resolution, the less the transmission measurements are affected by PVE, hence the smaller the biases in TBR. For soft-tissue tumors, as tumor and soft-tissue densities are similar, the transmission spatial resolution does not change the bias in TBR estimates.

The type of transmission map (high-resolution CT, segmented image or smoothed transmission scan) will therefore

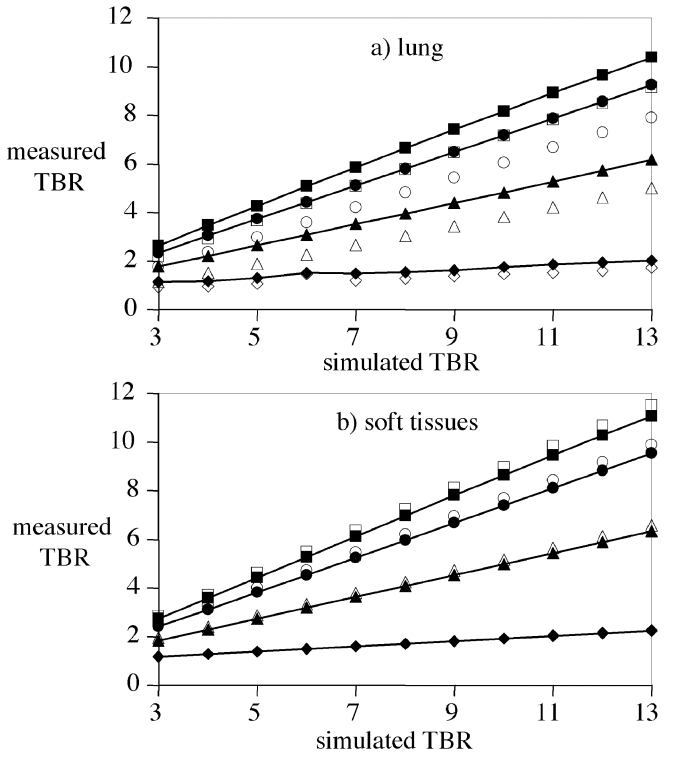

Fig. 7. Measured TBR with AC in (a) lung tumor; (b) soft-tissue tumor with $\mathrm{FWHM}_T = 8$ mm (empty symbol) and 4 mm (filled symbol) and $\mathrm{FWHM}_E = 4$ mm as a function of simulated TBR for lesion diameters of 4 cm (■), 2 cm (•), 1 cm (▲) and 0.5 cm (♦).

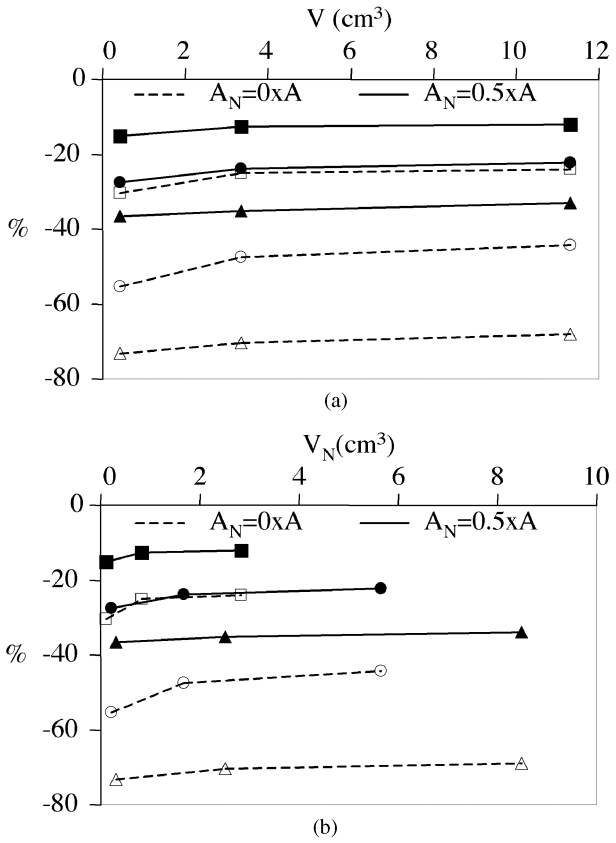

Fig. 8. Difference between average TBR measured over the whole tumor and average TBR that would be measured without necrosis with AC in a lung tumor with $\mathrm{FWHM} = 4$ mm as a function of a) tumor volume; b) necrosis volume for necrosis volume of $0.25 \times V$ (■), $0.5 \times V$ (•) and $0.75 \times V$ (▲).

affect TBR estimates for lung tumors but not for soft-tissue tumors. Indeed, lung tumors have a greater density than surrounding normal lung tissue, while soft-tissue tumors have a similar density as surrounding normal soft tissues. These results are consistent with previous results regarding the consequences of different emission and transmission resolutions [16] in cardiac PET.

E. Effect of Tumor Location

With AC, for a given TBR, biases in tumor uptake estimates were similar regardless the tumor location.

The comparison between NA and those having AC has demonstrated the efficiency of AC (Section III-C). As PVE does not depend on location for a given TBR, biases affecting TBR after AC are also independent of tumor location.

Recovery coefficients calculated for PVE correction of attenuation corrected images could therefore be the same for tumors located in the lung or in the soft tissues.

F. Effect of Tumor Nonuniformity

For a 33.5 cm^3 lung tumor ($D = 4$ cm) with $A = 2960$ kBq/ml including a 8.3 cm^3 inner necrotic region of activity half of that of the tumor ($A_N = 1480$ kBq/ml), the averaged TBR measured over the whole tumor was only 13% smaller than the averaged TBR that would be measured if the tumor had a uniform activity concentration with $\mathrm{TBR} = 10$. The TBR averaged over the whole tumor was underestimated by 12% with respect to the true TBR.

TABLE I
TBR UNDERESTIMATION AVERAGED OVER THE WHOLE TUMOR COMPARED WITH TBR UNDERESTIMATION OBSERVED FOR A UNIFORM TUMOR AS A FUNCTION OF NECROSIS-TO-TUMOR ACTIVITY AND VOLUME RATIOS

	V_N/V=0.25	V_N/V=0.5	V_N/V=0.75
A_N/A=0	from -30% to -24%	from -55% to -44%	from -74% to -67%
A_N/A=0.5	from -15% to -12%	from -27% to -22%	from -38% to -34%

The decrease in TBR values due to the presence of a necrotic core only depends on the necrosis-to-tumor volume ratio and on the necrosis-to-tumor activity ratio but does not depend on the tumor [Fig. 8(a)] and necrotic [Fig. 8(b)] volumes independently, nor on the necrosis and tumor activities independently. The difference between the measured TBR and the TBR that would be measured if no necrosis were present is also almost independent of background activity A_B. For example, for a 4.2–cm^3 tumor with $A_N = 0.5 \times A$ and $A = 1480$ kBq/ml, difference between the measured TBR and homogeneous TBR was -26.2% for $A_B = 296$ kBq/ml and -24.4% if $A_B = 148$ kBq/ml.

For a constant necrosis-to-tumor volume ratio, the more amplified the necrotic process (i.e., the smaller the necrosis-to-tumor activity ratio), the greater the difference between the measured TBR and the TBR which would be measured without necrosis (Table I and Fig. 8).

For a constant necrosis-to-tumor activity ratio, the larger the ratio of the necrotic volume over the tumor volume, the larger the difference between the measured TBR and the TBR that would be measured if no necrosis were present (Table I).

Assuming that at least a 15% TBR difference is needed for detecting a change in tumor metabolism, the percentage of necrotic volume that would make the necrosis process detectable depends on the necrosis-to-tumor activity ratio. For a necrosis-to-tumor activity ratio of 0.5, the necrosis would get detectable if the necrotic volume were at least 50% of the total tumor volume. For a necrosis-to-tumor activity ratio of 0, the necrosis would get detectable for a necrotic volume greater than 25% of the total tumor volume.

"Averaging" two TBR in a single anatomical ROI by considering an ROI encompassing nonuniform uptakes in the tumor makes it more difficult to detect necrosis. Our results give some insights into the volume of necrotic tissues needed to detect an overall change in TBR as a function of the amplitude of the necrotic process.

G. Relationship Between SUV and TBR

When assessing FDG PET images quantitatively, standardized uptake values (SUV) are often used to distinguish benign from malignant tumors. The SUV is a measure of local concentration of tracer divided by the injected dose normalized by the body weight [15]. For images corrected for attenuation, the percent biases in TBR presented in this paper are actually identical to the percent biases that would have been obtained had one considered SUV percent biases instead of TBR percent biases. Indeed, if one assumes that the denominator of the SUV expression is accurately estimated and that the background activity estimate is almost unbiased with AC, the percent bias in SUV is identical to the percent bias in TBR, as these two percent biases are identical to the percent bias in tumor uptake estimates. A study confirmed that considering SUV or TBR provides similar accuracy to differentiate malignant from benign pulmonary lesions with AC [12]. This identity between TBR percent biases and SUV percent biases does not hold for data not corrected for attenuation. Indeed, without AC, the SUV percent bias remains equal to the percent bias in tumor uptake but the TBR percent bias results from both the bias in tumor uptake and the bias in background uptake (no longer negligible because of attenuation). However, as SUV is never measured on images that are not corrected for attenuation, a study of the percent biases affecting SUV measured on data uncorrected for attenuation would not be relevant.

H. Methodological Limitations

Our simulations focussed on quantitative biases introduced by spatial resolution and attenuation and did not include the effects of noise, randoms, scatter, and cardiac and respiratory motions. We are currently investigating the impact of these effects upon our results using Monte Carlo simulations and data from phantoms and patients. Also, the ROIs used for TBR measurements were defined from the true contours of the simulated functional regions. Although it might be possible to draw such regions in the future thanks to the new PET/CT scanners, the actual impact of the ROI used for TBR measurements will have to be investigated, as there is currently no consensus regarding the ROI to be considered.

IV. Conclusion

Our study demonstrates that even when accurate AC is performed, tumor-to-background uptake ratios and SUVs are strongly underestimated because of limited spatial resolution. TBR and SUV underestimation up to 85% can be observed for a 5-mm tumor seen using a PET scanner with a 4-mm intrinsic spatial resolution. The impact of AC on TBR estimates depends both on tumor-to-surrounding tissues density and on tumor location, but the main trend is that TBR is systematically greater with AC than without for lung tumors, but not for soft-tissue tumors. When considering tumors with nonuniform uptakes the difference between measured TBR averaged over the whole nonuniform tumor and the TBR that would be measured if the tumor was uniform only depends on the necrosis-to-tumor volume and activity ratios, but not on the respective tumor and necrosis volumes and activities. When measuring the average tumor uptake over the whole tumor region (including the necrotic part), a TBR change greater than 15% was observed if the necrotic volume was at least 50% of the total tumor volume for a necrosis-to-tumor activity ratio of 0.5. The provided data regarding the impact of attenuation, lesion size, TBR, spatial resolution, and nonuniform uptake of the tumor upon TBR estimates should assist the quantitative interpretation of tumor-to-background uptake ratios and SUV in FDG PET.

References

[1] N. Avril, S. Bense, I. Ziegler, J. Dose, W. Weber, C. Laubenbacher, W. Römer, F. Jänicke, and M. Schwaiger, "Breast imaging with fluorine-18-FDG PET: Quantitative image analysis," *J. Nucl. Med.*, vol. 38, pp. 1186–1191, 1997.

[2] K. Higashi, T. Nishikawa, H. Seki, M. Oguchi, Y. Nambu, Y. Ueda, K. Yuasa, H. Tonami, T. Okimura, and I. Yamamoto, "Comparison of fluorine-18-FDG PET and thallium-201 SPECT in evalution of lung cancer," *J. Nucl. Med.*, vol. 39, pp. 9–15, 1998.

[3] V. J. Lowe, J. M. Hoffman, D. M. DeLong, E. P. Patz, and R. E. Coleman, "Semiquantitative and visual analysis of FDG-PET images in pulmonary abnormalities," *J. Nucl. Med.*, vol. 35, pp. 1771–1776, 1994.

[4] E. J. Hoffman, S. C. Huang, and M. E. Phelps, "Quantitation in positron emission computed tomography: 1 effect of object size," *J. Comput. Assist. Tomogr.*, vol. 3, pp. 299–308, 1979.

[5] R. M. Kessler, J. R. Ellis, and M. Eden, "Analysis of emission tomographic scan data: Limitations imposed by resolution and background," *J. Comput. Assist. Tomogr.*, vol. 8, pp. 514–522, 1984.

[6] R. L. Wahl, "To AC or not to AC: That is the question," *J. Nucl. Med.*, vol. 40, pp. 2025–2028, 1999.

[7] R. E. Coleman, C. M. Laymon, and T. G. Turkington, "FDG imaging of lung nodules: A phantom study comparing SPECT, camera-based PET, and dedicated PET," *Radiology.*, vol. 210, pp. 823–828, 1999.

[8] F. M. Bengel, S. I. Ziegler, N. Avril, W. Weber, C. Laubenbacher, and M. Schwaiger, "Whole-body positron emission tomography in clinical oncology: Comparison between attenuation-corrected and uncorrected images," *Eur. J. Nucl. Med.*, vol. 24, pp. 1091–1098, 1997.

[9] M. B. Imran, K. Kubota, S. Yamada, H. Fukada, K. Yamada, T. Fujiwara, and M. Itoh, "Lesion-to-background ratio in nonattenuation-corrected whole body FDG PET images," *J. Nucl. Med.*, vol. 39, pp. 1219–1223, 1998.

[10] I. G. Zubal, C. R. Harrell, and E. Smith, "Computerized three dimensional segmented human anatomy," *Med. Phys.*, vol. 21, pp. 299–302, 1994.

[11] H. Hudson and R. Larkin, "Accelerated image reconstruction using ordered subsets of projection data," *IEEE Trans. Med. Imag.*, vol. 13, pp. 601–609, Dec. 1994.
[12] S. B. Knight, D. Delbeke, J. R. Stewart, and M. P. Sandler, "Evaluation of pulmonary lesions with FDG-PET," *Chest*, vol. 109, pp. 982–988, 1996.
[13] F. Zito, M. C. Gilardi, P. Magnani, and F. Fazio, "Single-photon emission tomographic quantification in spherical objects: Effects of object size and background," *Eur. J. Nucl. Med.*, vol. 23, pp. 263–271, 1996.
[14] A. Kojima, M. Matsumoto, M. Takashi, Y. Hirota, and H. Yoshida, "Effect of spatial resolution in SPECT quantification values," *J. Nucl. Med.*, vol. 30, pp. 508–514, 1989.
[15] J. W. Keyes, "SUV: Standard uptake or silly useless value?," *J. Nucl. Med.*, vol. 36, pp. 1836–1839, 1995.
[16] S. R. Meikle, M. Dahlbom, and S. Cherry, "Attenuation correction using count-limited transmission data in positron emission tomography," *J. Nucl. Med.*, vol. 34, pp. 143–150, 1993.